

DEC 11 1943

6412.3  
+29  
62

NOT TO BE REMOVED FROM LIBRARY

TECHNICAL MEMORANDUMS

NATIONAL ADVISORY COMMITTEE FOR AERONAUTICS

NOT TO BE REMOVED FROM LIBRARY

NOT TO BE REMOVED FROM LIBRARY

-----  
No. 1054  
-----

HEAT TRANSFER AND HYDRAULIC FLOW RESISTANCE  
FOR STREAMS OF HIGH VELOCITY

By V. L. Lelchuk

Journal of Technical Physics  
Vol. IX, No. 9, 1939

LIBRARY  
NATIONAL ADVISORY COMMITTEE FOR AERONAUTICS  
LABORATORY  
Langley Field, Va.

Washington  
December 1943

*Haught Doc file*



3 1176 01441 5120

## NATIONAL ADVISORY COMMITTEE FOR AERONAUTICS

TECHNICAL MEMORANDUM NO. 1054

HEAT TRANSFER AND HYDRAULIC FLOW RESISTANCE  
FOR STREAMS OF HIGH VELOCITY\*

By V. L. Lelchuk

## SUMMARY

Problems of hydraulic flow resistance and heat transfer for streams with velocities comparable with acoustic have present great importance for various fields of technical science. Especially, they have great importance for the field of heat transfer in designing and constructing boilers of the "Velox" type. In this article a description of experiments and their results as regards definition of the laws of heat transfer in differential form for high velocity air streams inside smooth tubes are given.

## EXPERIMENTAL APPARATUS AND PROCEDURE

General Scheme of Experimental Apparatus  
and Experimental Section

The general scheme of experimental apparatus is shown in figure 1. The air came in from the compressor into the apparatus through the large surge tank B, which has the purpose of removing the pulsations and separating the water fog. The orifice D was installed to measure the air flow rate and the air passing through was directed into a zig zag conduit P inside of which there was an electric heater. The heated air passed through the mixing section of the pipe G into the experimental tube A where it lost a part of its heat to

---

\* Jour. Tech. Phys. (USSR), vol. IX, no. 9, 1939, pp. 808-818.

NOTE: Translation received from Massachusetts Institute of Technology, Cambridge, Mass.

cooling water which flowed through the casing around the experimental tube, losing its pressure and expanding up to the limit of atmospheric exhaust pressure. The air discharged from the experimental section at high velocity which approached acoustic velocity.

The experimental section is shown in figure 2. A smooth copper tube of 14-millimeter inside diameter and 16-millimeter outside diameter by 1431-millimeter length was placed axially inside a brass tube 19.8-millimeter inside diameter. The heated air flowed with high velocity through the inside tube and the cooling water flowed in the annular space. Transition from the large pipe to the experimental tube was accomplished smoothly by means of a slowly converging nozzle. A length of 21 millimeters at the exhaust end of the experimental tube was given a diverging conic shape. Thus the experimental tube may be considered as a nozzle, first converging and then after a long narrow throat, enlarging again. Flow velocities as high as acoustic velocity and corresponding pressure relations were achieved at the point of transition from the cylindrical section to the conic section. By this means the opportunity to make relatively easy all measurements, including even those in the acoustic region were obtained. The air pressure was measured at a number of points along the experimental section. The temperatures of the inside wall of the air tube as well as those of the cooling water were also measured along the flow. In the experimental tube 9 static pressure taps of 0.08-millimeter diameter were located to measure the changes in static pressure as the fluid flowed through the tube. In order to eliminate roughness formed by boring the pressure taps a special drill by which the burrs were cut off from inside the tube was made.

After the holes were made and the pressure taps attached the transverse section of the tube and its variation all along the length was measured by gradually filling the tube with mercury in the section between two pressure taps and weighing the mercury. The measurements showed that the diameter of the tube was sufficiently uniform all along. The average inside area of a transverse section of the tube was 155.3 square millimeters and the mean diameter 14.07 millimeters. At seven points in the outside wall of the copper tube thermocouples were inserted to measure the tube-wall temperatures and their variation along the tube. For this purpose small grooves

were made in the tube wall, the two thermocouple wires were inserted in the grooves and soldered over flush with the tube wall. In order to detect any asymmetry of cooling of the tube which might have occurred during the experiment, four thermocouples were inserted along a line parallel to the tube axis and three alternate couples were placed along a line diametrically opposite. The distances between the thermocouples can be seen in figure 1. To measure the temperature of the cooling water at points along the flow inside, thermocouples of wire of 0.2-millimeter diameters were placed in the annular space. The diameter of the smoothed soldered junctions was 1.0 millimeter. Each thermocouple was tied by a thin wire close to the experimental tube so that the free end of the couple was slightly above the tube surface. A thermocouple installed in this manner with relatively large thickness of junction equal to one-half the crack width assured measurement of the bulk temperature of the water flowing at this point. There were six such thermocouples along the tube in addition to two others to measure the inlet and exit temperatures of the water. These thermocouples were distributed similarly to the tube-wall thermocouples. All the thermocouples for measurement of the wall and water temperatures were carefully insulated by a special varnish and calibrated. The water thermocouple distribution in the annular space is shown in figure 1.

In making up the experimental section it was necessary to keep the experimental tube centered inside the casing to insure symmetrical flow of cooling medium. This was done by using, as spacers, three small wires 20-millimeters long and of diameter equal to the crack width soldered to the tube wall at each of these points. Besides, this, centering rings were soldered on each end of the experimental tube and the ends of the casing were then soldered to these rings. In order to avoid any deformation of the experimental section because of the differences in thermal expansion of experimental tube and casing, the latter was cut transversely in the middle into two sections. The ends of the casing could then move freely inside a metal ring placed over the cut in the casing. Tightening of the joint was accomplished by use of a rubber tube placed over the ring and wired to both ends of the cut casing; thus the rubber served to absorb all the deformation resulting from thermal expansion of tube and casing. The thermocouple leads were brought out through small holes in the casing. Short tubes of 3 millimeters outside-diameter were carefully soldered to the pressure taps in the test

section. These tubes were brought out through holes made in the casing as shown in figure 2 by short, thick-walled, metal-armored rubber tubes placed over the small tubes. A tube passing through and soldered to the casing was inserted into the outer end of the rubber. Thus there was assured the necessary compactness and elasticity of the joints to the manometer and all possible security in measurement of the static pressure of the air. To the outside wall of the casing there were also soldered five thermocouples to measure the casing temperature along the experimental section. The casing was insulated with asbestos to avoid heat loss.

#### Experimental Procedure and Measurements

Before the experiment was begun the air and the cooling water were started flowing in the apparatus and the electric heater was turned on to heat the whole apparatus and to reach steady-state operation. After the desired flow conditions were reached, the experiment was started. Before and during the experiment steady air flow rates were maintained by continuous observation of the level of the differential water manometer on the orifice and by careful regulation of the valve B. The duration of one experiment varied from 15 to 30 minutes. During this time all data were taken three times. Some of the experiments were repeated from two to three times under the same conditions. Because the air flow rates were regulated, the pressure in the experimental tube varied insignificantly during the experiment.

In order to assure even distribution of cooling water around the annular space, artificial turbulence was introduced into the water flow by admixture of compressed air which was put into the water line before the water entered the casing. The well-mixed air-water emulsion passed through the annular space at high velocity and thus during the experiments uniform smooth curves of thermocouple readings were obtained for the cooling water and the experimental tube. The inevitable inaccuracy in heat quantities due to the air in the water is insignificant even if the volume of the air were three times that actually used. In our experiments counter-current flow of air and cooling emulsion were used. With parallel flow the main portion of the change in water flow would occur in the first portion of the experimental section and this first section interests us least because it represents only the beginning of

the velocity range of interest. With counter-flow the change in water temperature is more uniform with insignificant concavity toward the axis of length. In this latter case the curve of water temperature from inlet to exit of the casing is almost linear along the entire experimental section. This assured greater accuracy in differentiation of these curves.

The distribution of air pressure along the flow was measured by a mercury differential manometer having 10 legs. A detailed description of this manometer is given in the work on measurement of hydraulic resistance. Nine legs of the manometer were attached to the pressure taps and the tenth point communicated to the atmosphere. Thus the differential manometer gave a distribution of mercury levels corresponding to the pressure gradient in the tube above atmospheric pressure. The air flow was measured by a standard orifice made of stainless steel placed in a 70-millimeter inside-diameter pipe upstream from the electric heater. The orifice diameter was 21 millimeters. The pressure drop across the orifice was measured by a U-tube manometer filled with colored water. The absolute pressure upstream from the orifice was measured by a precision Bourdon gage to six atmospheres with a scale graduated to 0.03 atmosphere. The air temperature upstream from the orifice was measured by a thermocouple.

The quantity of heat  $Q$  (per unit time) lost by the air in the test section was determined by measuring the weight rate of flow of cooling water and temperature rise of the water. In addition, the curve of water temperature against length of test section was measured so that by differentiation of this curve the instantaneous rate of heat transfer could be determined.

$$\frac{dQ}{dL} = \frac{cG_s \frac{dt_s}{dL}}{dL} \quad (1)$$

where

$G_s$  mass flow rate of water, kg/hr

$\frac{dt_s}{dL}$ \* derivative of water temperature  $t_s$  with respect to length, deg.C/meter

---

\*1 was changed to L in translation to facilitate reading the typewritten text.

$dQ/dL$  derivative of  $Q$  with respect to length in  
cal/(m)(hr)

$c$  specific heat of water = 1 cal/(g)(°C)

The entire heat loss from the air along the test section was also computed from measurement of air flow rates and inlet and exit temperature and pressure for the test section. With these mass flow rates and the same inlet and exit pressures and temperatures obtained in the 3-inch sections preceding and following the test section, the heat loss from the air was measured in a 3-inch inside-diameter pipe (where changes in kinetic energy of the air were negligible). The two independent measurements of  $Q$  checked in our experiments to within 5 percent.

#### EXPERIMENTAL DATA AND THEIR MEANING

In all our experiments at the exhaust end of the tube acoustic velocity at that temperature was attained. Table I shows the complete measured data for all experiments. From these data plots of measured quantities were made.

Figure 3 shows curves of the pressure distribution. The abscissa is marked as distance in millimeters from the entrance of the test section and the ordinate as the pressure in millimeters of water. For each experiment plots of temperatures of inside wall of test section, cooling water temperature, and casing wall temperature have been made and these are shown in figure 4.

The motion of a compressible gas is described by the following formulas:

(1) Conservation of matter

$$G = \frac{Fw}{V} \quad (2)$$

(2) Equation of state

$$pV = RT \quad (3)$$

(3) Energy balance

$$\frac{A w^2}{2g} + G_p T + Q = G_p T_o + A \frac{w_o^2}{2g} \quad (4)$$

where

G air flow rate, mass per unit time

F transverse area of tube

w flow velocity

V specific volume

p absolute pressure

T absolute temperature

w, V, P, T mean values over the section\*

Cp specific heat at constant pressure

R gas constant

A thermal equivalent of mechanical work

g acceleration of gravity

Q heat output per kilogram of air in the test section from the inlet to the section in question

Subscript:

o inlet section

If started at the large tube before the test section the initial kinetic energy  $A (w_o^2/2g)$  relative to  $C_p T_o$  can be neglected. In the author's experiments the quantities  $G/F$  and  $p$  were measured directly. In the large tube preceding the experimental section the inlet temperature of the air was measured by a resistance thermometer.

---

\*For the laws of averaging of the separate quantities, see the author's work on hydraulic resistance for high velocities.



The quantity  $Q$  may be calculated up to any section by the water mass flow rate and the temperature rise of the water.

From the plot of  $Q$  and the initial air temperature, the quantity so-called "stagnation temperature"  $T_m$  and its change along the test section have been computed

$$T_m = A \frac{w^2}{C_p 2g} + T = T_o - \frac{Q}{C_p} \quad (5)$$

A solution of equations (2) and (4) gives a quadratic equation for the flow temperature

$$T^2 = \frac{2gGp}{A} \left( \frac{F}{G} \frac{1}{R} \right)^2 p^2 T + \frac{2gC_p}{A} \left( \frac{F}{G} \frac{1}{R} \right)^2 p^2 T_m \quad (6)$$

To calculate  $T$  from equation (6) a graphical solution based on methods is described in the work on flow resistance. The magnitude of flow velocity is computed from the difference between stagnation and actual temperatures.

$$w = \sqrt{\frac{2gC_p}{A} (T_m - T)} \quad (7)$$

From the experiment friction factors have been calculated under conditions with heat flow. The Bernoulli equation for flow of compressible fluids

$$\frac{wdw}{g} = -V dp - \xi \frac{w^2}{2g} \frac{dL}{D} \quad (8)$$

together with equation (2) determines the friction factor  $\xi$  for compressible flow.

$$\xi = -2D \frac{d(p + \rho w^2)}{dL \rho w^2} \quad (9)$$

where

$\rho$   $1/Vg$  = air density

$D$  tube diameter

With very low velocities and  $\rho w^2 \ll p$  or  $w^2 \ll gpV = \frac{a^2}{k}$  (a acoustic velocity,  $k$  adiabatic exponent) — that is, with velocities far below acoustic, equation (9) becomes the ordinary relation for  $\xi$  for flow of incompressible fluids.

The quantity  $(p + \rho w^2)$  varied all along the tube in the experiment much less than did the quantities  $p$  and impact pressure  $\rho w^2$  separately. Therefore in calculating  $\xi$  from the experiments the curves of  $(p + \rho w^2)$  against tube length were differentiated. The values of  $\xi$  have been calculated for the sections  $L = 700, 900, 1100, 1250,$  and  $1360$  millimeters.

In figure 5 the experimental values of  $\xi$  as a function of Reynolds number, calculated on the mean stagnation temperature in a given section are shown as small circles. The curve fits the Nikuradse equation

$$\xi = 0.0032 + \frac{0.221}{Re^{0.237}} \quad (10)$$

So it is seen that the actual experiments with heat transfer occurring confirm the previous conclusion made for adiabatic streams — that is, that the Nikuradse relation for  $\xi$  is applicable to streams of high velocity.

In the same sections where the friction factors were determined, local heat transfer coefficients from the equation for heat flow for a tube surface element of diameter  $D$  and length  $dL$  were also computed

$$dQ = \alpha (T_m - T_{cm}) \pi D dL \quad (11)$$

where  $T_{cm}$  is the absolute temperature of the tube wall,

The values of  $dQ$  were calculated from experimental data by use of equation (1).

The utility of reckoning heat transfer coefficients, not on actual fluid temperature but on stagnation temperature, has already been well founded by Vittgeo (reference 2), M. F. Shirokov (reference 4), and Jung (reference 5). Calculation of the mean coefficient of heat transfer  $\bar{\alpha}$  was made for tube sections  $L = 0.7$  ( $L/D=50$ ) to  $L = 1.250M$ .

The curves of water and wall temperatures against tube length approximated straight lines in the section up to  $L = 1.250M$ ; therefore for stagnation temperature and for  $Q$  there also is, in this section, approximate linear dependency on length according to equations (5) and (1). To determine the mean  $\bar{\alpha}$  according to equation (11)

$$\bar{\alpha} = \frac{1}{L} \int_0^L \alpha \, dL = \frac{1}{\pi DL} \int_0^L \frac{dQ}{T_m - T_{cm}} \quad (12)$$

Substituting  $dQ = \alpha \, dL$ ,  $T_m - T_{cm} = \tau_0 - bL$ , where  $\alpha$ ,  $b$ ,  $\tau_0$  are constant, and after integration

$$\bar{\alpha} = \frac{Q}{\pi DL} \frac{1}{\tau_0 - \tau_L} \ln \frac{\tau_0}{\tau_L}$$

or

$$\bar{\alpha} = \frac{Q}{\pi DL \bar{\tau}} \quad (13)$$

where  $\bar{\tau} = T_m - T_{cm}$  is the temperature potential in a given section and

$$\bar{\tau} = \frac{\tau_0 - \tau_L}{\ln \frac{\tau_0}{\tau_L}}$$

is the logarithmic mean temperature difference in the tube between two transverse sections.

By use of equation (13) values of  $\alpha$  have been calculated for all these experiments as well as the dimensionless parameters Nu and Pe characterizing the heat transfer.

$$Nu = \frac{\alpha D}{\lambda} \quad (14)$$

$$Pe = \frac{w \gamma C_p D}{\lambda} \quad (15)$$

Here  $\lambda$  is the conductivity of the air.

The Reynolds-Prandtl hydrodynamic theory of heat transfer predicates a transfer of heat and momentum from the core of the stream to the walls by a process of turbulent eddy motion of the same stream particles. If, in this theory, the resistance to heat transfer of the thin laminar films for gases in tubes is neglected, the following relation between  $\alpha$  and  $\xi$  is obtained:

$$\alpha = w \gamma C_p \frac{\xi}{8}$$

or in dimensionless parameters,

$$\frac{Nu}{Pe} = \frac{\xi}{8} \quad (16)$$

As Shirokov has demonstrated, the hydrodynamic theory of heat transfer may be extended to streams of high velocities if for the transfer not only of the heat but also of equivalent kinetic energy from the core of the stream to the walls is allowed. Then equation (16) is valid if  $\alpha$  is calculated on the temperature difference based on stagnation temperature.

The data of these experiments confirm this relation and check with the data of Vittgeo (reference 2).

In figure 6 where the abscissa is  $Nu/Pe$  and the ordinate is  $\xi$  the experimental data for mean values along the test section are marked with small circles and the data of Vittgeio with triangles, the straight line is drawn as required by equation (16). It may be seen that over almost the whole range of this investigation, the data correlates well with equation (16) except in the small region of high values of  $Pe$ .

In figure 7 local values of  $Nu/Pe$  and  $\xi$  are marked. The solid straight line corresponds to equation (16) and the dotted line was fitted to the experimental data by the method of least squares. The conclusion regarding the dependency of  $Nu/Pe$  on  $\xi$  for mean values is also confirmed by figure 7.

Usually for gases, heat transfer experiments are reported as  $Nu$  against  $Pe$ , because  $\xi$  depends on  $Re$  and  $Re = Pe/Pr$  for gases is directly proportional to  $Pe$  (the Prandtl criterion  $Pr$  depends only on the number of atoms in the gas).

In figure 8  $Pe$  values are on the abscissa and  $Nu$  on the ordinate and the data based on mean values are shown as small circles. The values of the physical constants in  $Nu$  and  $Pe$  are calculated on mean gas stagnation temperature. It is to be noted that the data, calculated on stagnation temperature and not on limiting temperatures as is usually done in this field, fit well with the ten Bosch equation for air.

$$Nu = 0.0364 Pe^{0.75} \quad (17)$$

This is shown graphically on the same plot by the solid curve. This equation is obtained by substitution in equation (16) for  $\xi$  by the relation of Blasius which fits the Nikuradse equation for  $Re \leq 100,000$  and it is confirmed by multiple experiments at low velocities if the physical properties are based on the wall temperature.

This is also shown in figure 9 where the small circles show the relation between the local values of  $Nu$  and  $Pe$  calculated on stagnation temperature and the solid curve corresponds to the ten Bosch formula.

It should be stated that these experiments have not shown any noticeable influence of temperature on  $\alpha$  and

$\xi$  as has been reported by Jung on stack gases where the temperature variation of the gases was much greater than in our experiments.

### CONCLUSIONS

1. The relations for friction and heat transfer for cooling hot air streams flowing at velocities up to acoustic velocity through straight water-cooled tubes have been studied experimentally.

2. The range of variables covered values of Nusselt numbers, —Nu from 200 to 500, Peclet numbers —Pe from 50,000 to 300,000, and Reynolds numbers —Re from 70,000 to 420,000; the air temperature varied from 400° C at the inlet to 140° C at the exit, and the velocities reached the acoustic value (up to 420M/sec) at the exit end of the tube.

3. It was found that within the limits of our experiments, the calculation of heat transfer coefficients based on stagnation temperatures confirmed the relation,

$$\frac{Nu}{Pe} = \frac{\xi}{8}, \text{ which is derived from the Reynolds-Prandtl}$$

analogy. This is as well confirmed for mean values of Nu and Pe in the tube as for point values of Nu and Pe and is by no means dependent on the (Bairstow) Mach number (the ratio of stream velocity to acoustic velocity).

4. The values of  $\xi$  for flow with heat transfer fit the Nikuradse formula as well as  $\xi$  for streams without heat transfer.

$$\xi = 0.0032 + \frac{0.221}{Re^{0.237}}$$

Translation by N. P. Vakar  
and G. C. Williams.

## REFERENCES

1. Lelchuk, V. L.: Jour. Tech. Phys. (USSR), vol. 7, 1826, 1937.
2. Vittgeo: Jour. Tech. Phys. (USSR), vol. 5, no. 10, 1935.
3. Jung, Ingvar: Transmission of Heat and Frictional Resistance by Gas Flow in Pipes at High Velocities. Forschungsheft 380, vol. 7, 1936.
4. Shirokov, M. F.: Bull. Federal Heat Science Institute. No. 9, 107, 1935.





Table I

16

NACA Technical Memorandum No. 1054

Run	Static air pressure in mm H <sub>2</sub> O										Mass rate of flow of air kg/sec	Air temperature in °C		Mass rate of flow of cooling water in kg/sec
	Before test section	At distance of										Before test section	Behind test section	
		203.5	453.5	703.5	953.5	1203.5	1353.5	1394.0	1404	1410				
		mm from pipe inlet												
1	24,740	19,187	17,926	16,489	14,807	12,706	10,739	9,682	9,153	8,285	0.0486	341	171	0.0306
2	24,900	19,323	18,062	16,611	14,916	12,706	10,780	9,736	9,221	8,340	.0486	345	175	.0306
3	24,900	19,296	18,048	16,597	14,889	12,773	10,753	9,709	9,092	8,326	.0486	353	178	.0302
4	21,075	16,028	14,970	13,777	12,326	10,539	8,855	7,987	7,529	6,875	.0393	381	190	.0278
5	21,075	16,353	15,323	14,062	12,598	10,780	9,072	8,190	7,743	7,092	.0395	392	193	.0282
6	-----	22,740	21,276	19,608	17,628	15,201	12,774	11,540	10,957	9,940	.0582	338	182	.0411
7	42,800	33,358	31,382	28,869	25,995	22,428	18,808	16,923	15,987	14,523	.0893	254	149	.0417
8	43,000	33,846	31,800	29,236	26,279	22,632	18,888	16,950	15,974	14,550	.0894	247	145	.0406
9	49,500	39,039	36,612	33,738	30,392	26,225	21,832	19,581	18,523	16,828	.1042	231	140	.0382
10	49,700	39,388	37,019	34,063	30,673	26,429	21,927	19,649	18,577	16,869	.1047	231	140	.0375
11	50,100	38,036	35,731	33,046	29,805	25,707	21,615	19,432	18,428	16,746	.1028	231	142	.0382
12	50,100	36,775	34,456	31,785	28,666	24,643	20,571	18,388	17,425	15,838	.0998	231	142	.0389
13	36,800	28,828	26,971	24,882	22,397	19,336	16,162	14,730	39,953	12,620	.0736	284	155	.0413

Table I-Continued

Run	Cooling water temperature in °C								Temperature of test section of outer pipe wall in °C								Temperature of outer wall jacket in °C				
	At outlet of jacket	at distance of						At inlet of jacket	at distance of							at distance of					
		416	670	913	1173	1330	1406		416	667	912	1177	1335	1375	1406	323.5	673.5	829.5	1083.5	1293.5	
		mm from pipe inlet							mm from pipe inlet							mm from pipe inlet					
1	75.3	53.3	45.0	28.6	20.0	13.6	13.8	7.8	66.0	49.0	37.9	30.0	22.0	19.2	19.4	52.0	39.0	27.4	16.8	9.2	
2	73.1	54.1	46.5	29.8	20.8	14.2	14.2	8.4	66.1	50.0	38.6	32.0	22.8	20.0	20.3	54.0	41.1	27.7	16.9	9.9	
3	75.6	55.8	48.8	31.8	22.2	15.5	16.0	9.6	68.8	52.8	41.6	33.4	24.4	21.6	22.2	55.1	40.7	28.4	17.6	9.7	
4	75.5	57.2	49.0	32.5	22.6	15.8	16.2	9.8	71.0	55.0	42.5	33.5	24.2	21.7	22.5	58.4	42.8	30.0	18.6	11.0	
5	77.8	59.0	49.2	32.4	22.9	15.8	16.8	9.8	70.0	53.1	41.4	34.4	24.4	22.0	21.8	59.1	44.1	31.6	19.6	11.0	
6	64.7	47.1	39.6	26.4	19.2	13.9	14.1	9.4	60.8	43.8	33.6	28.4	21.4	19.0	19.0	48.4	36.6	26.4	17.4	11.0	
7	63.0	47.7	40.0	26.3	19.2	13.2	13.6	8.8	59.7	44.4	34.5	28.2	22.0	19.0	18.6	47.9	36.5	26.0	16.8	10.2	
8	63.4	48.6	41.3	27.2	19.9	13.8	14.0	9.0	61.1	45.2	35.8	29.2	22.6	19.3	18.8	49.6	37.6	26.7	13.6	11.1	
9	68.4	51.7	43.8	29.2	21.2	14.5	14.7	9.1	64.2	47.6	37.6	31.1	23.8	20.2	19.8	53.4	40.7	29.0	18.8	11.2	
10	66.5	52.0	44.2	29.0	21.5	14.7	14.8	9.0	64.7	48.0	38.6	31.3	24.0	20.0	19.8	53.5	40.8	29.5	19.0	11.6	
11	64.8	50.4	43.4	29.0	20.8	14.1	14.5	8.8	62.2	46.8	37.3	31.0	23.7	20.1	20.0	52.1	40.2	28.9	18.8	11.4	
12	64.2	49.2	41.7	27.9	20.0	13.6	14.0	8.8	61.2	45.8	36.2	29.8	23.1	20.0	19.6	50.5	38.6	28.0	18.4	11.2	
13	63.0	43.8	38.1	22.6	21.6	13.1	15.6	8.0	64.6	46.8	46.0	39.4	30.2	24.0	23.5	45.0	31.3	21.7	14.2	10.3	

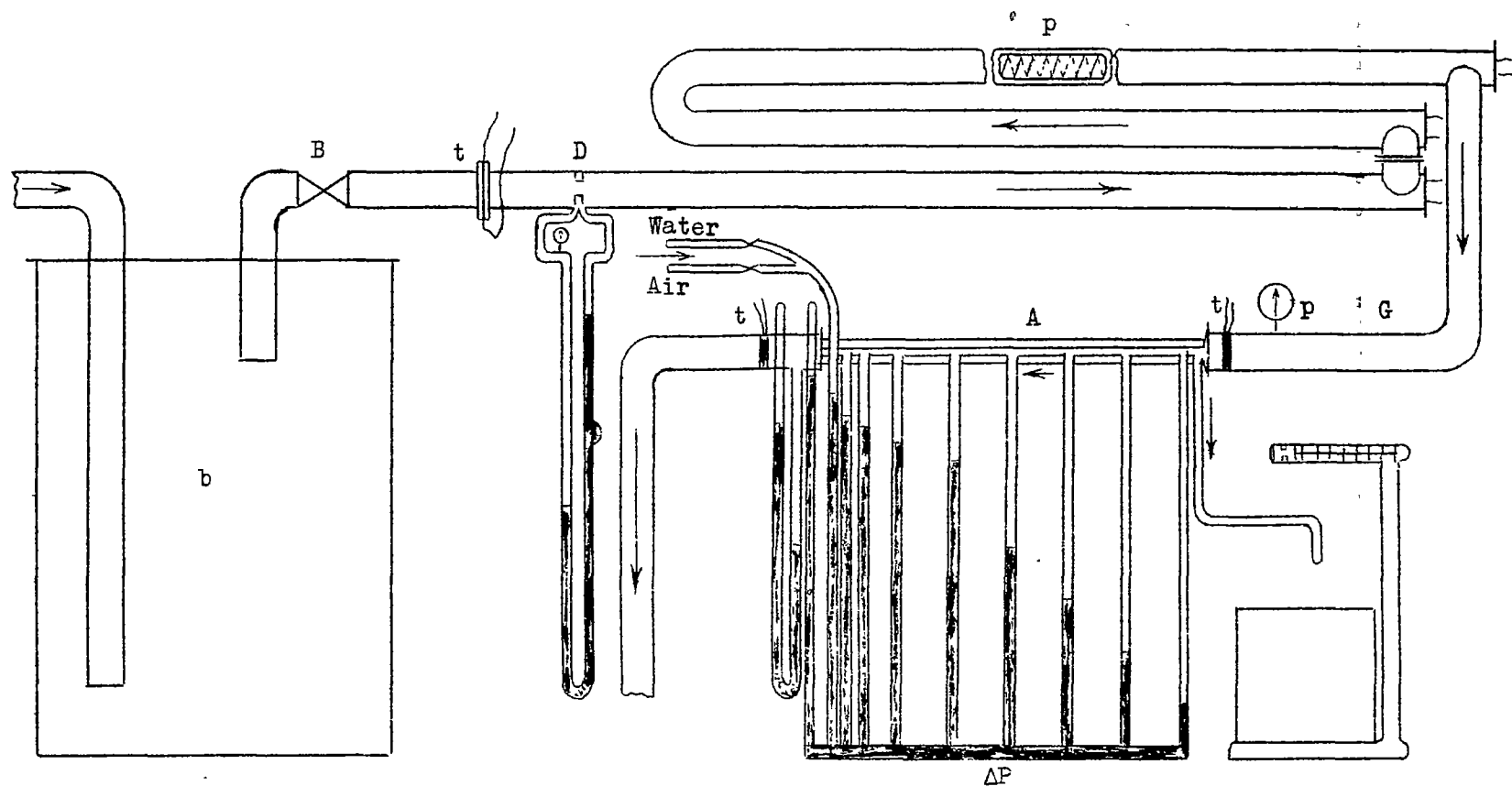


Figure 1.- Scheme of experimental apparatus.

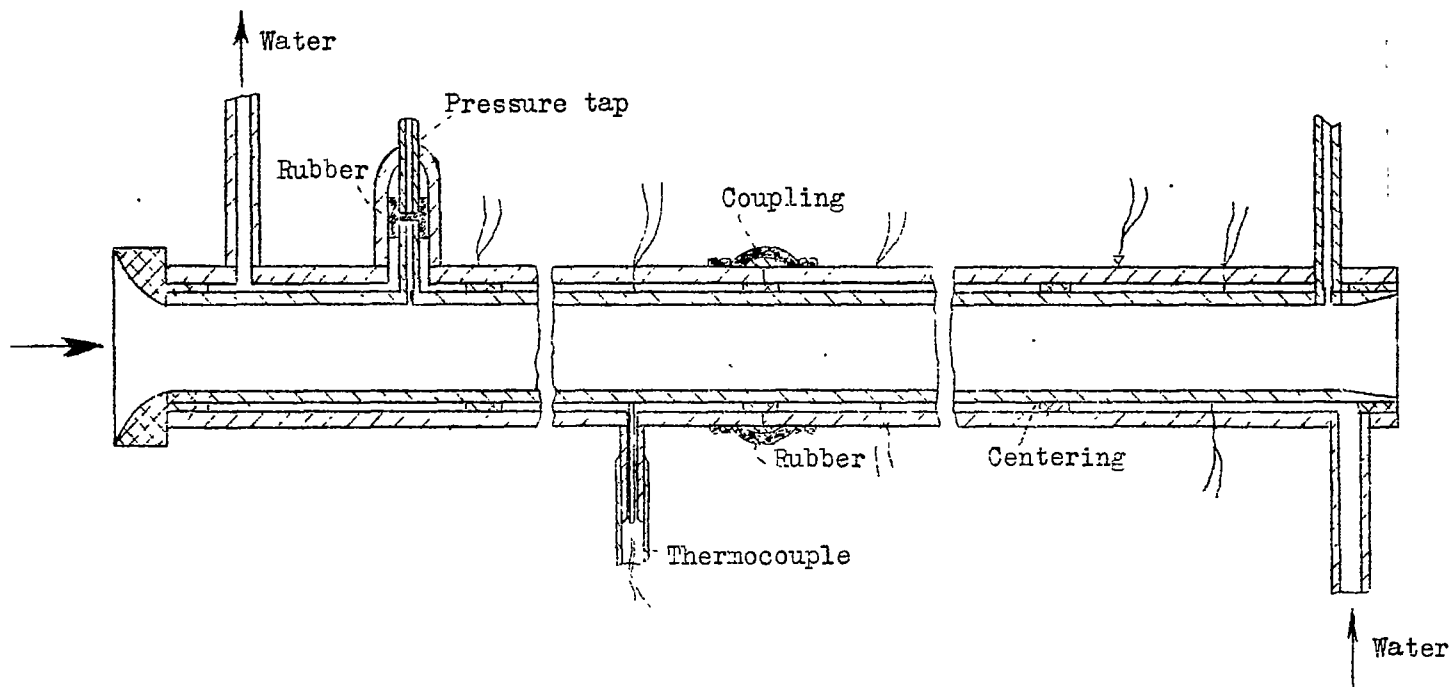


Figure 2.- Scheme of experimental tube.

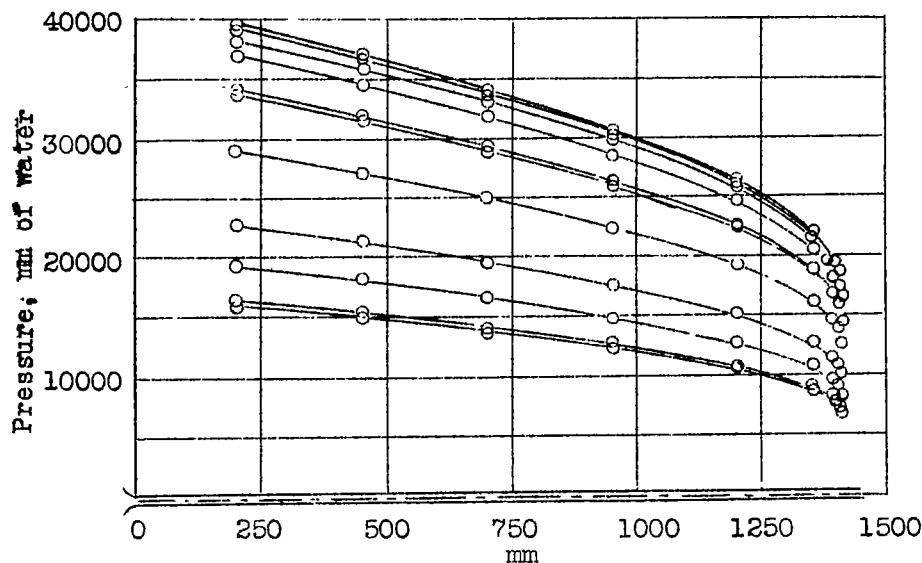


Figure 3.- Pressure distribution along experimental tube.

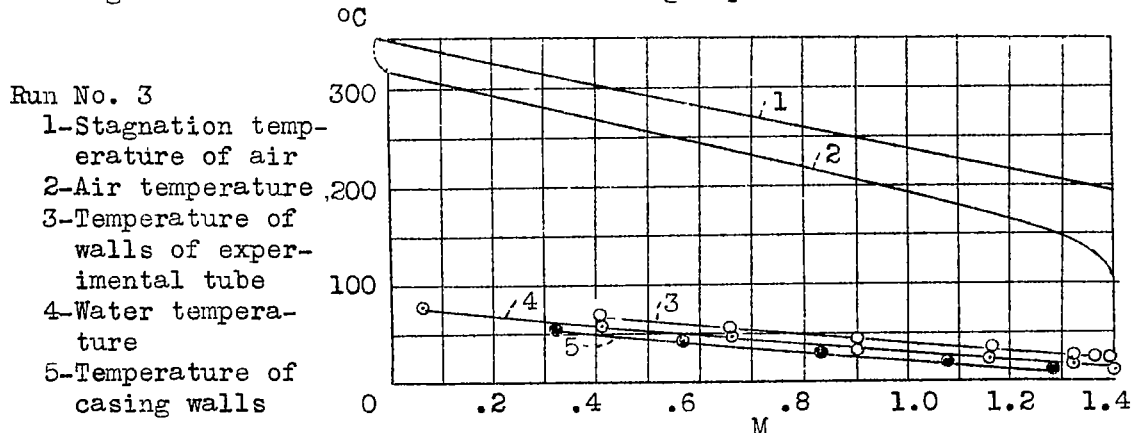


Figure 4.- Temperature distribution along experimental tube.

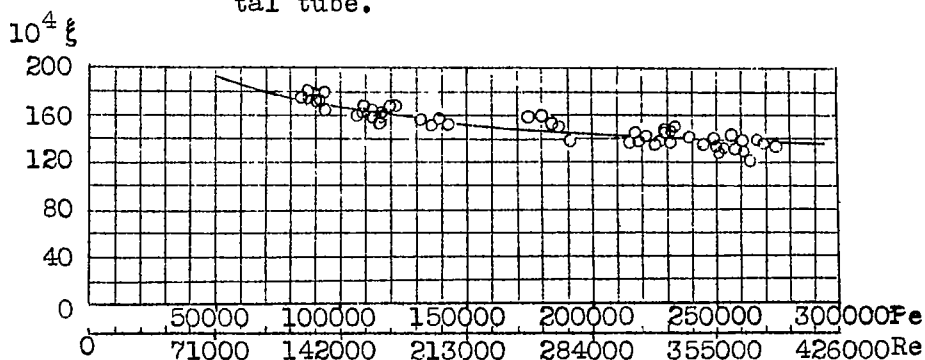


Figure 5

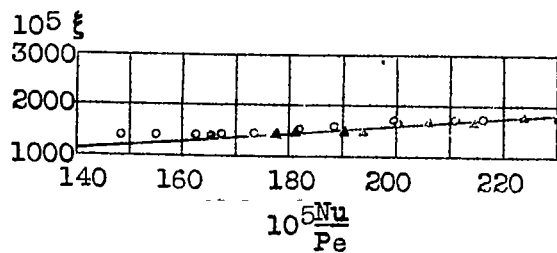


Figure 6

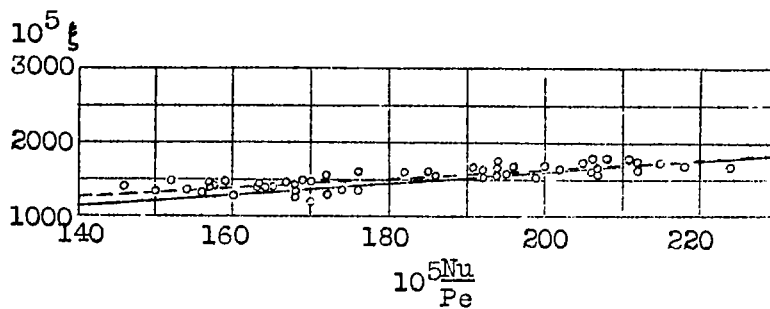


Figure 7

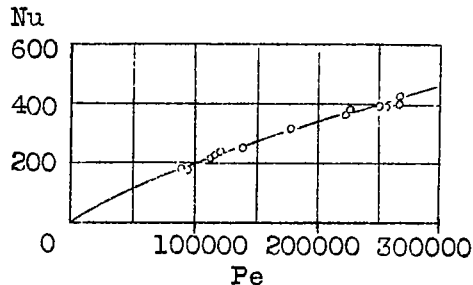


Figure 8

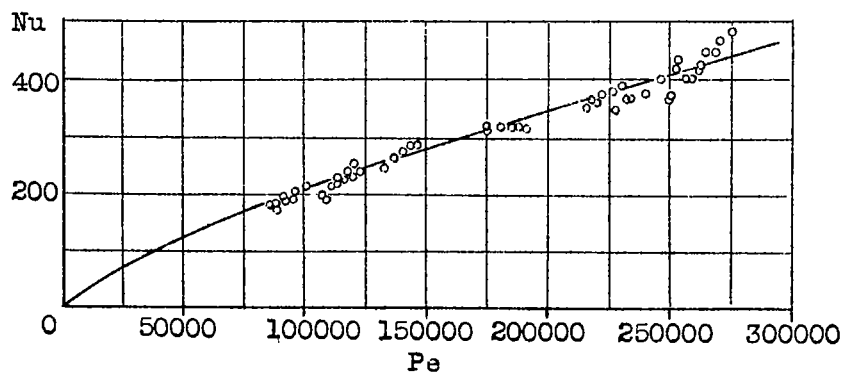


Figure 9

NASA Technical Library



3 1176 01441 5120